Supporting Information for: Photo-induced tip-sample forces for chemical nano-imaging and spectroscopy

Brian T. O'Callahan,* Jun Yan, Fabian Menges, Eric A. Muller, and Markus B. Raschke†

Department of Physics, Department of Chemistry, and JILA,

University of Colorado at Boulder, Boulder, CO 80309

(Dated: July 27, 2018)

*Present address: brian.ocallahan@pnnl.gov

†Electronic address: markus.raschke@colorado.edu

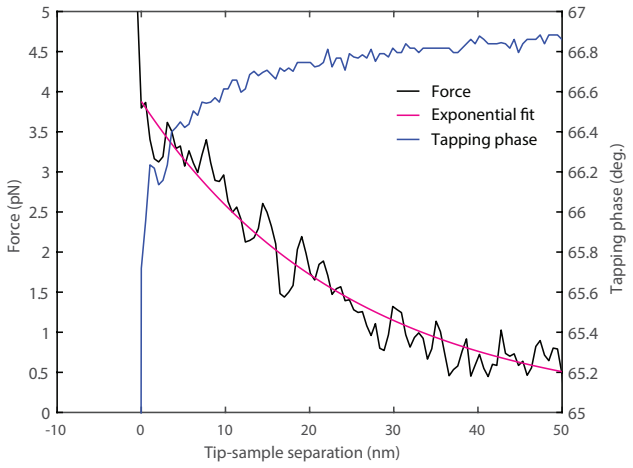

Fig. S 1: Detail of force approach curve over a 60-nm thick PMMA film shown in Figure 4a) of the main text. The measured force (black) shows a long-range behavior that can be fit to an exponential (magenta). The corresponding tapping phase (blue) shows a slight decrease, indicating a repulsive force.

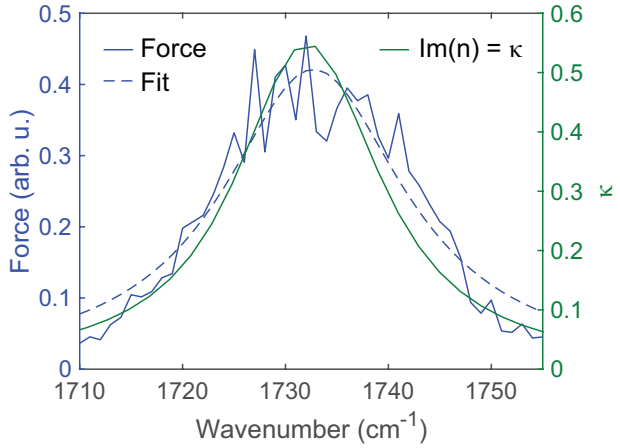

Fig. S 2: Spectrum of the long-range force acquired 15 nm above a 60-nm thick PMMA film (blue, solid), and corresponding Lorentzian fit (blue, dashed). Spectrum of the imaginary part of the complex index of refraction (green). The qualitative agreement suggests that the long-range force is related to sample absorption, instead of the optical gradient force.

Fig. S1 shows a zoom-in of the long-range force behavior over a 60-nm thick PMMA film from Fig. 4a) of the main text decaying exponentially, with a corresponding decrease in tapping phase. This decrease in the tapping phase indicates that the force is repulsive.

Fig. S2 shows the spectrum of the long-ranged force measured at a distance of 15 nm

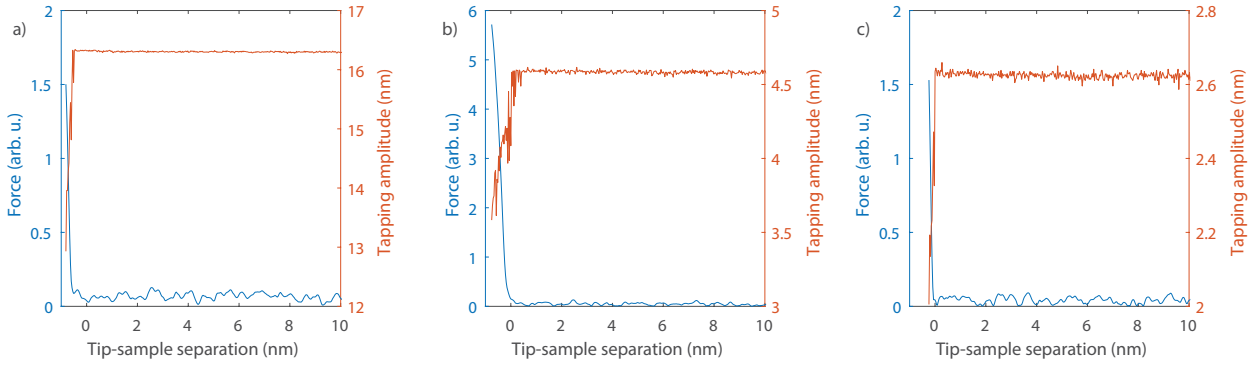

Fig. S 3: Force approach curves of a $\sim$ 40 nm thick PMMA film with free-space tapping amplitudes of a) $\sim$ 16 nm, b) $\sim$ 4.6 nm, and c) $\sim$ 2.6 nm.

above a 60-nm thick PMMA film, which resembles the spectral behavior of κ.

Fig. S3 shows three approach curves on a PMMA film with thickness of $\sim$ 40 nm, acquired for three different values of tapping amplitudes. The 40 nm thickness is less than the film thickness of the sample used in Fig. 4 of the main text, in order to reduce the effect of the sample thermal expansion, and the associated photo-acoustic force, while still generating an appreciable optical gradient force. Small tapping amplitudes were used to increase interaction time with the expected short range optical gradient force, which is predicted to be confined to within a few nm above the sample surface, which should further increase the sensitivity. However, even with tapping amplitudes as small as 2.6 nm (peak-to-peak), the signal is dominated by thermal expansion confined to tip-sample contact, with no detectable long-range force observed.

I. MODEL

In the dipole approximation, we treat the sample as a semi-infinite half-space with a planar interface and we model the tip as a sphere of radius r with polarizability $\alpha_{\rm t} = 4\pi r^3 \epsilon_0 \frac{\epsilon_{\rm t}-1}{\epsilon_{\rm t}+2}$, where $\epsilon_{\rm t}$ is the dielectric function of the tip [1, 2]. When the tip is close to a sample surface, the tip dipole p induces an polarization in the sample here treated as an image dipole of strength $p' = p\beta$, where $\beta = \frac{\epsilon_s(\omega)-1}{\epsilon_s(\omega)+1}$ and $\epsilon_s(\omega)$ is the dielectric function of the sample. The electric field at the tip position is the sum of the incident electric field and the field due to the image dipole $E = E_0 + \frac{\beta p}{16\pi\epsilon_0(r+h)^3}$ where h is the separation between the bottom of the sphere and the sample surface. The field due to the image dipole acts back

on to the tip dipole and repolarizes it, giving a modified, coupled tip-sample polarization of $p = \alpha_t \left(E_0 + \frac{\beta p}{16\pi\epsilon_0 (r+h)^3} \right)$, where the second term is the radiation reaction term. We can describe the tip-sample mutual response by solving the recursive relation for p, and assigning the system an effective polarizability α_{eff} given by $\alpha_{\text{eff}} = p/E_0 = \frac{\alpha_t}{(1-\beta\alpha_t/16\pi\epsilon_0(r+h)^3)}$. The field acting on the tip dipole is given by $E = E_0 + \frac{\beta\alpha_{\text{eff}} E_0}{16\pi\epsilon_0(r+h)^3}$ and the force experienced by the tip is then given by:

$$\vec{F} = \vec{p} \cdot \nabla \vec{E} = \text{Re}\left(\alpha_{\text{eff}}^2 \frac{3E_0^2}{16\pi\epsilon_0 (r+h)^4} \right). \tag{1}$$

Past predictions of the optical force have differed from the above treatment by considering the sample as a sphere with polarizability $\alpha_{\text{s}} = 4\pi r^3 \epsilon_0 \frac{\epsilon_{\text{s}}-1}{\epsilon_{\text{s}}+2}$ instead of as a semi-infinite half-space as well as neglecting the radiation reaction term between the two spheres [3]. This results in the following expression for the optical gradient force:

$$F = \vec{p_t} \cdot \nabla \vec{E} = -\frac{1}{2}\text{Re}\left(\frac{1}{4\pi\epsilon_0} \frac{6\alpha_t \alpha_s^* E^2}{z^4} \right) \propto \text{Re}(\alpha_t \alpha_s^*) \frac{E^2}{z^4} \propto (\alpha_t' \alpha_s' + \alpha_t'' \alpha_s'') \frac{E^2}{z^4}. \tag{2}$$

While the electric field at the tip position was given by $E = E_0 + \frac{\alpha_{\text{s}} E_0}{2\pi\epsilon_0 (2r+h)^3}$, the strength of the tip dipole was given by $p_{\text{t}} = \alpha_{\text{t}} E_0$ and neglected the additional electric field contribution due to the sample dipole.

Calculations using Eq. 1 and Eq. 2 both show dispersive spectral lineshapes, however the inconsistent model presented previously which results in Eq. 2 underestimates the force magnitude by close to an order of magnitude. Eq.1 is based on the more accurate sample geometry, and is based on a self-consistent model.

For the thickness dependent measurements, our samples consist of a PMMA layer of thickness t on a Si substrate creating a air/PMMA/Si structure. To describe this layered system, we use an effective dielectric function derived from the boundary conditions across the two interfaces given by [4]:

$$\epsilon_*(\omega, q) = \epsilon_P(\omega) \frac{\epsilon_S(\omega) k_P^z(\omega, q) - \epsilon_P(\omega) k_P^z(\omega, q) \tanh(i k_P^z(\omega, q) t)}{\epsilon_P(\omega) k_S^z(\omega, q) - \epsilon_S(\omega) k_P^z(\omega) \tanh(i k_P^z(\omega) t)}. \tag{3}$$

Here, $\epsilon_{P,S}(\omega)$ refer to the dielectric functions of PMMA and Si, respectively, and $k_{P,S}^z(\omega, q) = \sqrt{\epsilon_{P,S}(\omega)\omega^2/c^2 - q^2}$ is the z-component of the wavevector in PMMA and Si, respectively.

Figure 4 shows the topographic image of the tapered PMMA film used for the thickness dependence measurements displayed in Fig. 3 of the main text, with linecut indicated by the red dashed line. While our model describing the thickness dependence of the thermal expansion force (Eq. 3 of the main text) neglects the spatial variation of the film thickness

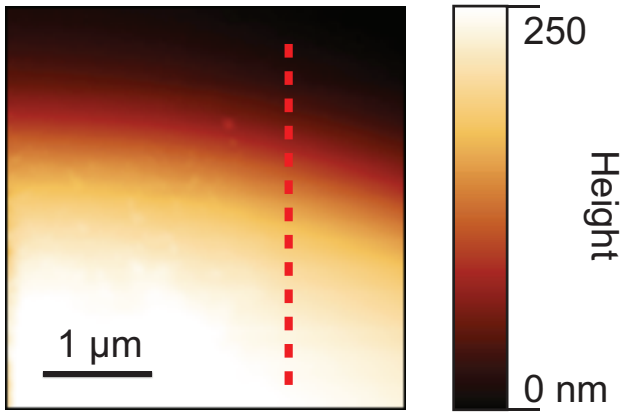

Fig. S 4: Topography image of the tapered PMMA film used for the thickness dependence study. Red dashed line indicates the approximate location of the linecut used for the data displayed in Fig. 3 of the main text.

across the scan region, since the tip apex radius is much smaller than the laser focus, the sample expands uniformly in the surface normal direction at the apex location. Thus the film thickness directly below the tip apex primarily determines the thermal expansion distance, with negligible perturbation due to surface inhomogeneities.

---

[1] B. Knoll and F. Keilmann, Opt. Commun. **182**, 321 (2000).

[2] J. M. Atkin, P. M. Sass, P. E. Teichen, J. D. Eaves, and M. B. Raschke, J. Phys. Chem. Lett. **6**, 4616 (2015), https://doi.org/10.1021/acs.jpclett.5b02093.

[3] D. Nowak, W. Morrison, H. K. Wickramasinghe, J. Jahng, E. Potma, L. Wan, R. Ruiz, T. R. Albrecht, K. Schmidt, J. Frommer, et al., Sci. Adv. **2**, e1501571 (2016).

[4] L. M. Zhang, G. O. Andreev, Z. Fei, A. S. McLeod, G. Dominguez, M. Thiemens, A. H. Castro-Neto, D. N. Basov, and M. M. Fogler, Phys. Rev. B **85**, 075419 (2012).